Thermal state truncation by using quantum scissors device

Hong-xia Zhao[1], Xue–xiang Xu[2,†], Hong-chun Yuan[3]
[1]*Information Engineering college,*
Jiangxi University of technology, Nanchang 330098, China
[2]*Center for Quantum Science and Technology,*
Jiangxi Normal University, Nanchang 330022, China
[3]*College of Electrical and Optoelectronic Engineering,*
Changzhou Institute of Technology,
Changzhou 213002, China
[†]*Corresponding author: xxxjxnu@gmail.com*

arXiv:1607.06919v1 [quant-ph] 23 Jul 2016

A non-Gaussian state being a mixture of the vacuum and single-photon states can be generated by truncating a thermal state in a quantum scissors device of Pegg et al. [Phys. Rev. Lett. 81 (1998) 1604]. In contrast to the thermal state, the generated state shows nonclassical property including the negativity of Wigner function. Besides, signal amplification and signal-to-noise ratio enhancement can be achieved.

PACS: 42.50,Dv, 03.67.-a, 05.30.-d, 03.65.Wj
Keywords: quantum scissor; thermal state; signal amplification; signal-to-noise ratio; Wigner function; parity

I. INTRODUCTION

The generation of quantum states is a prerequisite for universal quantum information processing (QIP) [1]. Quantum states are usually classified into discrete-variable (DV) and continuous-variable (CV) descriptions [2]. In the CV quantum regime, there are two classes of quantum states that play an important role in QIP: Gaussian and non-Gaussian states, referring to their character of wave function or Wigner function [3, 4]. In general, Gaussian states are relatively easy to generate and manipulate using current standard optical technology[5].

However, in the recent several decades, some probabilistic schemes are proposed to generate and manipulate non-Gaussian states [6–8]. Many schemes work in postselection [9], that is, the generated state is accepted conditionally on a measurement outcome. The typical examples include photon addition and subtraction [10], and noise addition [11]. Among them, an interesting scheme was based on the quantum-scissors devices. In 1998, Pegg, Phillips and Barnett proposed this quantum state truncation scheme, which change an optical state $\gamma_0 |0\rangle + \gamma_1 |1\rangle + \gamma_2 |2\rangle + \cdots$ into qubit optical state $\gamma_0 |0\rangle + \gamma_1 |1\rangle$. The device is then called a quantum scissors device (QSD), while the effect is referred to as optical state truncation via projection synthesis. This quantum mechanical phenomenon was actually a nonlocal effect relying on entanglement because no light from the input mode can reach the output mode [12]. After its proposal, an experiment of quantum scissors was realized by Babichev, Ries and Lvovsky [13] by applying the experimentally feasible proposal of Ref. [14–16]. The QSD was also applied and generalized to generate not only qubits but also qutrits [17] and qudits [18, 19] of any dimension. Similar quantum state can be also generated via a four-wave mixing process in a cavity [20].

Following these works on QSD, Ferreyrol et al. implemented a nondeterministic optical noiseless amplifier for a coherent state [21]. Moreover, heralded noiseless linear amplifications were designed and realized [22–24]. Recently, an experimental demonstration of a practical nondeterministic quantum optical amplification scheme was presented to achieve amplification of known sets of coherent states with high fidelity [25]. By the way, many systems transmitting signals using quantum states could benefit from amplification. In fact, any attempt to amplify signal must introduce noise inevitably. In other words, perfect deterministic amplification of an unknown quantum signal is impossible. In addition, Miranowicz et. al. studied the phase-space interference of quantum states optically truncated by QSD [26].

Inspired by the above works, we generate a non-Gaussian mixed state by using a Gaussian thermal state as the input state of the quantum scissors in this paper. This process transform an input thermal state into an incoherent mixture of only zero-photon and single-photon components. The success probability of such event is studied. Some properties of the generated state, such as signal amplification, signal-to-noise ratio and the negativity of the Wigner function, are investigated in detail. The paper is organized as follows. In section II, we outline the framework of QSD and introduce the scheme of thermal state truncation. Quantum state is derived explicitly and the probability is discussed. Subsequently, some statistical properties, such as average photon number, intensity gain, signal-to-noise ratio, are investigated in section III. In addition, we study the Wigner function and the parity for the output state in section IV. Conclusions are summarized in the final section.

II. THERMAL STATE TRUNCATION SCHEME

In this section, we outline the basic framework of quantum scissors device and introduce our scheme of thermal state truncation.

A. Framework of quantum scissors device

QSD mainly includes two beam splitters (BSs) and three channels, as shown in Fig.1. Three channels are described by the optical modes a, b, and c in terms of their respective creation (annihilation) operators $a^{\dagger}(a)$, $b^{\dagger}(b)$ and $c^{\dagger}(c)$. Since every channel have an input port and an output port, the QSD have six ports. The interaction including several key stages as follows. Firstly, the channel a and the channel c are correlated through an asymmetrical beam splitter (A-BS), whose operation can be described by the unitary operator $B_1 = e^{\theta\left(a^{\dagger}c - ac^{\dagger}\right)}$ with the transmissivity $T = \cos^2\theta$. After that, the channel b and the channel c are then correlated through another symmetrical beam splitter (S-BS, also 50:50 BS), whose operation can be described by the unitary operator $B_2 = e^{\frac{\pi}{4}\left(b^{\dagger}c - bc^{\dagger}\right)}$. Moreover, among these six ports, four ports are fixed with special processes as follows: (1) Injecting the auxiliary single-photon $|1\rangle$ in the input port of channel a; (2) Injecting the auxiliary zero-photon $|0\rangle$ in the input port of channel c; (3) Detecting the single-photon $|1\rangle$ in the output port of channel b; and (4) Detecting the zero-photon $|0\rangle$ in the output port of channel c.

QSD leaves only one input port (i.e., the input port in channel b) and one output port (i.e., the output port in channel a). Injecting an appropriate input state in the input port, one can generate a new quantum state in the output port. Many previous theoretical and experimental schemes have used the pure states as the input states to generated quantum states. Here, our proposed scheme use a mixed state as the input state to generate quantum state.

B. Thermal state truncation

Using a mixed state (i.e., thermal state) as the input state, we shall generate another mixed state in our present protocol. The input thermal state is given by

$$\rho_{th} = \sum_{n=0}^{\infty} \frac{\bar{n}^n}{(\bar{n}+1)^{n+1}} |n\rangle\langle n|, \tag{1}$$

where $\bar{n}$ is the average number of the thermal photons [27]. Therefore, the output generated state can be expressed as

$$\begin{aligned}\rho_{out} &= \frac{1}{p_d}\langle 0_c|\langle 1_b| B_2\{\rho_{th}\otimes \\ &\quad [B_1(|1_a\rangle\langle 1_a|\otimes|0_c\rangle\langle 0_c|)B_1^{\dagger}]\}B_2^{\dagger}|1_b\rangle|0_c\rangle \end{aligned} \tag{2}$$

where p_d is the success probability.

The explicit density operator in Eq.(2) can further be expressed as

$$\rho_{out} = p_0|0\rangle\langle 0| + p_1|1\rangle\langle 1|, \tag{3}$$

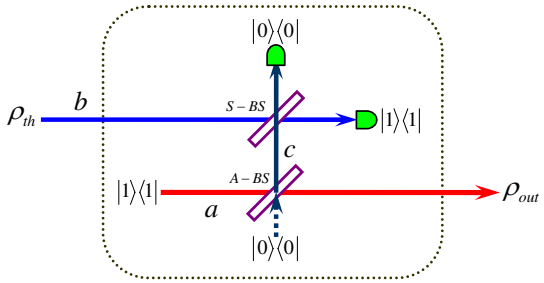

FIG. 1: (Colour online) Conceptual scheme of "quantum scissors device" (QSD) for thermal state truncation. The auxiliary single-photon $|1\rangle\langle 1|$ in channel a and the auxiliary single-photon $|0\rangle\langle 0|$ in channel c generates an entangled state between the modes a and c after passing through an asymmetrical beam splitter (A-BS) with the transmissivity T. The input mode b (accompanied by the input thermal state ρ_{th}) is then combined with c in a (50:50) symmetrical beam splitter (S-BS). A successful heralded truncation (accompanied by the output generated state ρ_{out}) in the output a mode is flagged by a single-photon event in the output b mode detection and no photons on the output c mode detection.

where $p_0 = (1-T)(\bar{n}+1)/(\bar{n}+1-T)$ and $p_1 = \bar{n}T/(\bar{n}+1-T)$ are, respectively, the zero-photon distribution probability and the one-photon distribution probability. Obviously, the output state is an incoherent mixture of a vacuum state $|0\rangle\langle 0|$ and a one-photon state $|1\rangle\langle 1|$ with certain ratio coefficients p_0, p_1. If $T = 0$, then $\rho_{out} \to |0\rangle\langle 0|$; while for $T = 1$, then $\rho_{out} \to |1\rangle\langle 1|$.

From another point of view, the output generated state in Eq.(3) remains only the first two terms of the input thermal state in Eq.(1), which can also be considered as an truncation from the input thermal state. However, the corresponding coefficients of these terms are changed. Moreover, the output generated state carry the information of the input thermal state because it also depend on the thermal parameter $\bar{n}$. Since no light from the input port reaches the output port, this process also mark the nonlocal quantum effect of the operation for the quantum scissors.

From present protocol, we easily obtain p_d as follows

$$p_d = \frac{\bar{n}+1-T}{2(\bar{n}+1)^2}. \tag{4}$$

For a given $\bar{n}$, it can be shown that p_d is a linear decreasing function of T.

In Fig.2, we plot p_d as a function of T for different $\bar{n}$. For instance, when $\bar{n} = 1$, we have $p_d|_{\bar{n}=1} = 0.25 - 0.125T$ (see the green line in Fig.2); when $\bar{n} = 0$, we have $p_d|_{\bar{n}=0} = 0.5 - 0.5T$ (see the black line in Fig.2). The results on the success probability provide a theoretical reference for experimental realization.

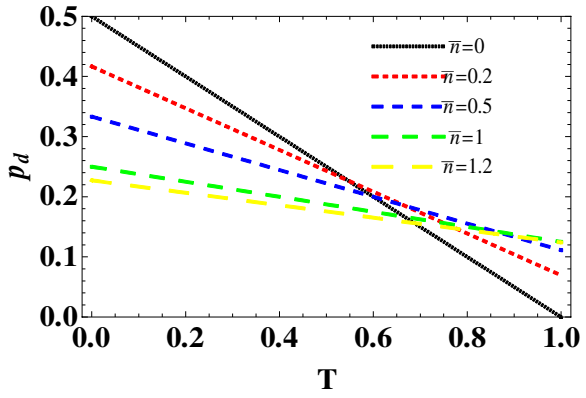

FIG. 2: (Colour online) Probability of successfully generating the output state as a function of the beam-splitter transmissivity according to the model presented in the text. The average photon number of the input thermal state $\bar{n}$ has been fixed to 0, 0.2, 0.5, 1, 1.2.

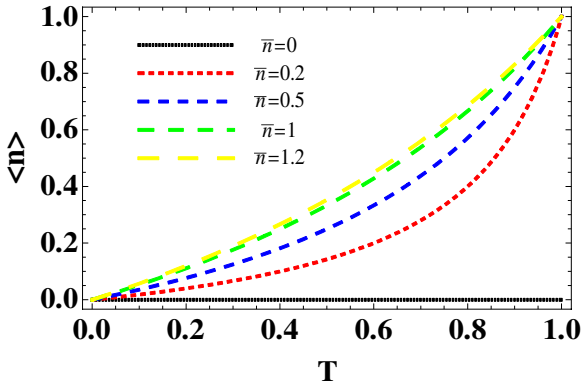

FIG. 3: (Colour online) Average photon number of the output state as a function of the beam-splitter transmissivity. The average photon number of the input thermal state $\bar{n}$ has been fixed to 0, 0.2, 0.5, 1, 1.2.

III. STATISTICAL PROPERTIES OF THE GENERATED STATE

By adjusting the interaction parameters, i.e., the thermal parameter $\bar{n}$ of the input state and the transmission parameter T of the A-BS, one can obtain different output states with different figures of merits. Some statistical properties, such as average photon number, intensity gain and signal-to-noise ratio, are studied in this section. As the reference, we will compare the properties of the output state with those of the input state.

A. Average photon number and intensity gain

Using the definition of the average photon number, we have $\langle\hat{n}\rangle_{\rho_{th}} = \bar{n}$ for the input thermal state and

$$\langle\hat{n}\rangle_{\rho_{out}} = \frac{\bar{n}T}{\bar{n}+1-T}. \tag{5}$$

for the output generated state. Here $\hat{n}$ is the operator of the photon number [28].

In Fig.3, we plot $\langle\hat{n}\rangle_{\rho_{out}}$ as a function of T for different $\bar{n}$. Two extreme cases, such as, e.g. (1) $\langle\hat{n}\rangle_{\rho_{out}} \equiv 0$ if $\bar{n} = 0$ or $T = 0$, and (2) $\langle\hat{n}\rangle_{\rho_{out}} \equiv 1$ if $T = 1$ for any $\bar{n} \neq 0$, are always hold. No matter how large the input thermal parameter $\langle\hat{n}\rangle_{\rho_{th}}$ is, there always exists $\langle\hat{n}\rangle_{\rho_{out}} \in [0, 1]$. Moreover, $\langle\hat{n}\rangle_{\rho_{out}}$ is an increasing function of T for a given nonzero $\bar{n}$.

In order to describe signal amplification, we define the intensity gain as $g = \langle\hat{n}\rangle_{\rho_{out}} / \langle\hat{n}\rangle_{\rho_{th}}$, which is related with the intensity $\langle\hat{n}\rangle_{\rho_{out}}$ of the output field with that ($\langle\hat{n}\rangle_{\rho_{th}}$) of the input field. Therefore we have

$$g = \frac{T}{\bar{n}+1-T}. \tag{6}$$

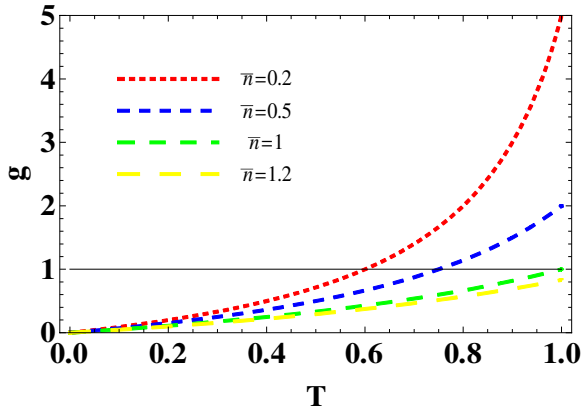

FIG. 4: (Colour online) Intensity gain of the output state as a function of the beam-splitter transmissivity. The average photon number of the input thermal state $\bar{n}$ has been fixed to 0.2, 0.5, 1, 1.2. Here the amplification (i.e., $g > 1$) occur only for $\bar{n} < 1$ and $T > (\bar{n}+1)/2$. There exist no amplification for high-intensity ($\bar{n} > 1$) thermal state.

If $g > 1$, then there exist signal amplification.

Fig.4 shows the intensity gain g as a function of T for different $\bar{n}$. If $\bar{n} \geq 1$, g is impossible to exceed 1, which means no amplification. In other words, the amplification happens only for the cases $\bar{n} < 1$ with $T \in ((\bar{n}+1)/2, 1]$.

B. Signal to noise ratio

Signal-to-noise ratio (abbreviated SNR or S/N) is a measure used in science and engineering that compares the level of a desired signal to the level of background noise [29]. Here we are interesting to the effect that the process has on the noise of these states. Typically this is shown by calculating the variance of

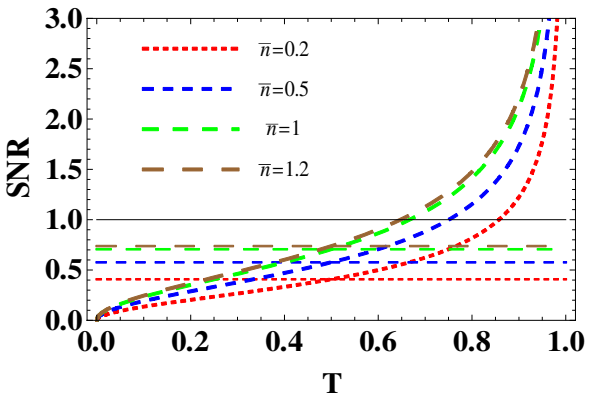

FIG. 5: (Colour online) Signal to noise ratio of the output states (curve line) as a function of the beam-splitter transmissivity, compared to their corresponding thermal states (straight line). Here $\bar{n}$ has been fixed to 0.2, 0.5, 1, 1.2. A clear enhancement for a given $\bar{n}$ can be seen for values of $T > 0.5$. the SNR higher than 1:1 (black line) can be found in lager $T > (\bar{n}+1)/(2\bar{n}+1)$.

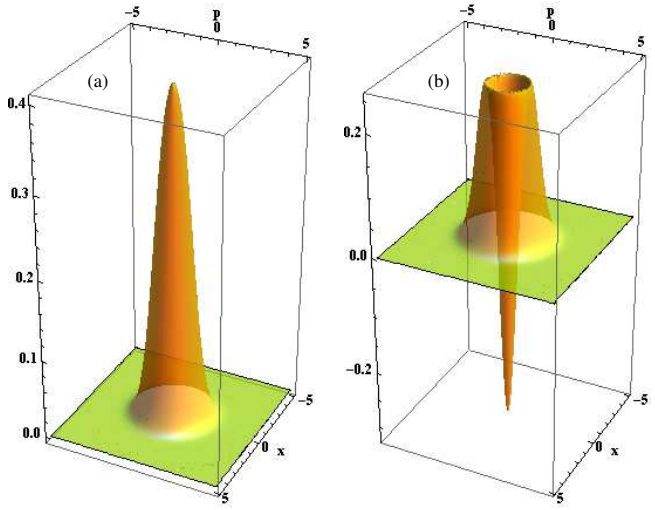

FIG. 6: (Colour online) Wigner function of the output state with (a) $\bar{n} = 0.5$, $T = 0.4$ and (b) $\bar{n} = 0.5$, $T = 0.9$. Case (b) has the negaive region.

the photon number and forming the SNR, defined by $SNR = \langle\hat{n}\rangle / \sqrt{\langle\hat{n}^2\rangle - \langle\hat{n}\rangle^2}$. From the definition, we have $\langle\hat{n}\rangle|_{\rho_{th}} = \bar{n}$, $\langle\hat{n}^2\rangle|_{\rho_{th}} = \bar{n} + 2\bar{n}^2$, and then $SNR|_{\rho_{th}} = \bar{n}/\sqrt{\bar{n}+\bar{n}^2}$ for the input thermal state ρ_{th}. While for our generated state ρ_{out}, we find $\langle\hat{n}\rangle|_{\rho_{out}} = \langle\hat{n}^2\rangle|_{\rho_{out}} = p_1$ and

$$SNR|_{\rho_{out}} = \sqrt{\frac{\bar{n}T}{(1-T)(\bar{n}+1)}}. \tag{7}$$

As is shown in Fig.5, we see the SNR for the output states, as compared to their corresponding thermal states, of the same fixed average photon number. It is found that a clear enhancement (corresponding to its input thermal state) can be seen for $T > 0.5$. Moreover, although the SNR of the input thermal state is always smaller than 1:1, the SNR higher than 1:1 for the output generated state can be found in larger T ($> (\bar{n}+1)/(2\bar{n}+1)$).

IV. WIGNER FUNCTION AND PARITY OF THE GENERATED STATE

The negative Wigner function is a witness of the nonclassicality of a quantum state [30–32]. For a single-mode density operator ρ, the Wigner function in the coherent state representation $|z\rangle$ can be expressed as $W(\beta) = \frac{2e^{2|\beta|^2}}{\pi}\int \frac{d^2z}{\pi}\langle -z|\rho|z\rangle e^{-2(z\beta^*-z^*\beta)}$, where $\beta = (q+ip)/\sqrt{2}$. Therefore we easily obtain $W_{\rho_{th}}(\beta) = 2/(\pi(2\bar{n}+1))e^{-2|\beta|^2/(2\bar{n}+1)}$ for the input thermal state and

$$W_{\rho_{out}}(\beta) = p_0 W_{|0\rangle\langle 0|}(\beta) + p_1 W_{|1\rangle\langle 1|}(\beta) \tag{8}$$

for the output generated state with $W_{|0\rangle\langle 0|}(\beta) = \frac{2}{\pi}e^{-2|\beta|^2}$ and $W_{|1\rangle\langle 1|}(\beta) = \frac{2}{\pi}(4|\beta|^2 - 1)e^{-2|\beta|^2}$.

As we all know, the thermal state is a Gaussian state, whose Wigner function have no negative region. However, our output generated states have lost the Gaussian characters because of the non-Gaussian forms of their Wigner functions. In addition, the Wigner function will exhibit negative in some region satisfying the following condition $|\beta|^2 < [2T\bar{n} - (\bar{n}+1-T)]/(4\bar{n}T)$. In Fig.6, we plot the Wigner functions of the output generated states for two different cases, where the negative region is found for case with large T.

Since the Wigner function of the output state is symmetrical in x and p space, one can determine the fact whether the Wigner function have negative region by seeing $W_{\rho_{out}}(\beta = 0)$. As Gerry pointed out that the Wigner function at the origin is the expectation value of the parity operator $\Pi = (-1)^{\hat{n}}$, that is $\langle\Pi\rangle = \frac{\pi}{2}W(0)$ [33]. Thus, we have $\langle\Pi\rangle_{\rho_{th}} = 1/(2\bar{n}+1)$ for the input thermal state and

$$\langle\Pi\rangle_{\rho_{out}} = \frac{\bar{n}+1-T-2T\bar{n}}{\bar{n}+1-T}, \tag{9}$$

for the output generated state. Fig.7 show $\langle\Pi\rangle_{\rho_{out}}$ as a function of T for different $\bar{n}$.

Photon number states are assigned a parity of $+1$ if their photon number is even and a parity of -1 if odd [34]. According to Eq.(3), we verify $\langle\Pi\rangle_{\rho_{out}} = p_0 - p_1$. If the condition $T > (\bar{n}+1)/(1+2\bar{n})$ is hold, then there exist $\langle\Pi\rangle_{\rho_{out}} < 0$, which means that the Wigner function must exhibit negative region in the phase space.

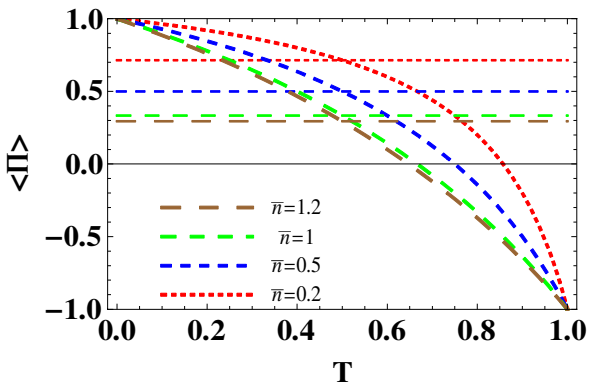

FIG. 7: (Colour online) Parity of the output state **as a function of the beam-splitter transmissivity**, where $\bar{n}$ has been fixed to 0.2, 0.5, 1, 1.2. The negative region of the Wigner function can be seen for values of $T > (\bar{n}+1)/(1+2\bar{n})$.

V. CONCLUSION

In summary, we have applied the QSD of Pegg, Philips and Barnett to truncate a thermal field to a completely mixed qubit state, i.e., a mixture of the vacuum and single-photon state. The explicit expression was derived in Schrodinger picture and the success probability of such event was discussed. The output generated state depend on two interaction parameters, i.e., the input thermal parameter and the transmissivity of the A-BS. It is shown that the success probability is a linear decreasing function of the transmissivity for any given input parameter. Some nonclassical properties of the qubit state were analyzed including intensity amplification, singal-to-noise ratio, and the non-positive Wigner function. It was shown that the average photon number of the output state can be adjusted between 0 and 1. The intensity amplification will happen only for small-intensity thermal field ($\bar{n} < 1$) and large-transmissivity ($T > (\bar{n}+1)/2$). The SNR of the output state can be enhanced by the operation for a given input thermal state at larger values of T (> 0.5). The SNR higher than unity can be found in the range of $T > (\bar{n}+1)/(2\bar{n}+1)$. In addition, the negativity of the Wigner function appears only for proper $T > (\bar{n}+1)/(1+2\bar{n})$.

Acknowledgments

We would like to thank Li-yun Hu and Bi-xuan Fan for their great helpful discussions. This work was supported by the Research Foundation of the Education Department of Jiangxi Province of China (Nos. GJJ151150 and GJJ150338) and the Natural Science Foundation of Jiangxi Province of China (20151BAB202013) as well as the National Natural Science Foundation of China(Grants No. 11264018 and No. 11447002).

Appendix A: Derivation of the density operator in Eq.(3)

In this appendix, we provide a detailed process of deriving the explicit expression of the output generated state in Schrodinger picture. Substituting $|1_a\rangle = \frac{d}{ds_1}e^{s_1 a^\dagger}|0_a\rangle|_{s_1=0}$, $\langle 1_a| = \frac{d}{dh_1}\langle 0_a|\exp e^{h_1 a}|_{h_1=0}$, $|1_b\rangle = \frac{d}{ds_2}e^{s_2 b^\dagger}|0_b\rangle|_{s_2=0}$, $\langle 1_b| = \frac{d}{dh_2}\langle 0_b|e^{h_2 b}|_{h_2=0}$, as well as

$$\rho_{th} = \frac{1}{\bar{n}}\int \frac{d^2\alpha}{\pi} e^{-(\frac{1}{\bar{n}}+1)|\alpha|^2} e^{\alpha b^\dagger}|0_b\rangle\langle 0_b| e^{\alpha^* b},$$

into Eq.(2), we have

$$\begin{aligned}\rho_{out} = & \frac{d^4}{\bar{n}p_d ds_1 dh_1 dh_2 ds_2} \\ & \int \frac{d^2\alpha}{\pi} e^{-(\frac{1}{\bar{n}}+1)|\alpha|^2}\langle 0_c|\langle 0_b| e^{h_2 b} \\ & e^{s_1 t a^\dagger + \frac{\alpha - s_1 r}{\sqrt{2}}b^\dagger - \frac{\alpha + s_1 r}{\sqrt{2}}c^\dagger}|0_a\rangle|0_b\rangle|0_c\rangle \\ & \langle 0_c|\langle 0_b|\langle 0_a| e^{h_1 t a + \frac{\alpha^* - h_1 r}{\sqrt{2}}b - \frac{\alpha^* + h_1 r}{\sqrt{2}}c} \\ & e^{s_2 b^\dagger}|0_b\rangle|0_c\rangle|_{s_1=s_2=h_1=h_2=0}\end{aligned}$$

where we have used the following transformations

$$\begin{aligned} B_1 a B_1^\dagger &= at - cr, \quad B_1 c B_1^\dagger = ar + ct, \\ B_2 b B_2^\dagger &= \frac{b-c}{\sqrt{2}}, \quad B_2 c B_2^\dagger = \frac{b+c}{\sqrt{2}}. \end{aligned}$$

and $B_1|0_a\rangle|0_c\rangle = |0_a\rangle|0_c\rangle$, $B_2|0_b\rangle|0_c\rangle = |0_b\rangle|0_c\rangle$, as well as their conjugations. In addition, $t = \cos\theta$ and $r = \sin\theta$ are the transmission coefficient and the reflection coefficient of the A-BS, respectively. After detailed calculation, we obtain

$$\begin{aligned}\rho_{out} = & \frac{d^4}{(\bar{n}+1)p_d ds_1 dh_1 dh_2 ds_2} \\ & e^{\frac{\bar{n}}{2(\bar{n}+1)}s_2 h_2 - \frac{r}{\sqrt{2}}(h_1 s_2 + r h_2 s_1)} \\ & e^{s_1 t a^\dagger}|0_a\rangle\langle 0_a| e^{h_1 t a}|_{s_1=s_2=h_1=h_2=0}\end{aligned}$$

Using $|0_a\rangle\langle 0_a| = :e^{-a^\dagger a}:$ and making the derivative in the normal ordering form (denoted by $:\cdots:$), we have

$$\rho_{out} =: \left(p_0 + p_1 a^\dagger a\right)\exp\left(-a^\dagger a\right):$$

Thus the density operator in Eq.(3) is obtained.

[1] P. Kok, B. W. Lovett, Introduction to Optical quantum information Processing, Cambridge University Press, New York, 2010.

[2] M. A. Nielseen, I. L. Chuang, Quantum computation and quantum information, Cambridge University Press, New York, 2000.
[3] U. L. Andersen, G. Leuchs, C. Silberhorn, Laser Photon. Rev. 4 (2010) 337.
[4] S. L. Braunstein, P. van Loock, Rev. Mod. Phys. 77 (2005) 513.
[5] X. B. Wang, T. Hiroshima, A. Tomita, M. Hayashi, Phys. Rep. 448 (2007) 1.
[6] F. Dell'Anno, S. D. Siena, F. Illuminati, Phys. Rep. 428 (2006) 53.
[7] U. L. Andersen, J. S. Neergaard-Nielsen, P. van Loock, and A. Furusawa, nature phys. 11 (2015) 713.
[8] A.I. Lvovsky, J. Mlynek, Phys. Rev. Lett. 88 (2002) 250401.
[9] T. C. Ralph and A. P. Lund, in proceeding of the 9th International Conference on Quantum Communication Measurement and Computing, edited by A. Lvovsky, AIP, Melville, New York, 2009.
[10] M. S. Kim, J. Phys. B: At. Mol. Opt. Phys. 41 (2008) 133001.
[11] P. Marek, R. Filip, Phys. Rev. A 81 (2010) 022302.
[12] D. T. Pegg, L. S. Phillips, S. M. Barnett, Phys. Rev. Lett. 81 (1998) 1604.
[13] S. A. Babichew, J. Ries, A. I. Lvovsky, Europhys. Lett. 64 (2003) 1.
[14] S. K. Ozdemir, A. Miranowicz, M. Koashi, N. Imoto, Phys. Rev. A 64 (2001) 063818.
[15] S. K. Ozdemir, A. Miranowicz, M. Koashi, N. Imoto, Phys. Rev. A 66 (2002) 053809.
[16] S. K. Ozdemir, A. Miranowicz, M. Koashi, N. Imoto, J. Mod. Opt. 49 (2002) 977.
[17] M. Koniorczyk, Z. Kurucz, A. Gabris, J. Janszky, Phys. Rev. A 62 (2000) 013802.
[18] A. Miranowicz, S. K. Ozdemir, J. Bajer, M. Koashi, N. Imoto, J. Opt. Soc. Am. B 24 (2007) 379.
[19] A. Miranowicz, J. Opt. B: Quantum Semiclass. Opt. 7 (2005) 142.
[20] B. X. Fan, Z. L. Duan, L. Zhou, C. H. Yuan, Z. Y. Ou, W. P. Zhang, Phys. Rev. A 80 (2009) 063809.
[21] F. Ferreyrol, M. Barbieri, R. Blandino, S. Fossier, R. Tualle-Brouri, P. Grangier, Phys. Rev. Lett. 104 (2010) 123603.
[22] G. Y. Xiang, T. C. Ralph, A. P. Lund, N. Walk, G. J. Pryde, Nature Photon. 4 (2010) 316.
[23] C. I. Osorio, N. Bruno, N. Sangouard, H. Zbinden, N. Gisin, R. T. Thew, Phys. Rev. A 86 (2012) 023815.
[24] Y. Li, A. R. R. Carvalho, M. R. James, Phys. Rev. A 93 (2016) 052312.
[25] R. J. Donaldson, R. J. Collins, E. Eleftheriadou, S. M. Barnett, J. Jeffers, G. S. Buller, Phys. Rev. Lett. 114 (2015) 120505.
[26] A. Miranowicz, M. Paprzycka, A. Pathak, F. Nori, Phys. Rev. A 89 (2014) 033812.
[27] C. C. Gerry, P. Knight, Introductory quantum optics, Cambridge University Press, New York, 2005.
[28] M. O. Scully, M. S. Zubairy, Quantum Optics, Cambridge University Press, New York, 1997.
[29] M. A. Choma, M. V. Sarunic, C. Yang, J. A. Izatt, Opt. Exp. 11 (2003) 2183.
[30] A. Kenfack, K. Zyczkowski, J. Opt. B, Quantum Semiclass. Opt. 6 (2004) 396.
[31] X. X. Xu, H. C. Yuan, Phys. Lett. A 380 (2016) 2342.
[32] H. L. Zhang, H. C. Yuan, L. Y. Hu, X. X. Xu, Opt. Commun. 356 (2015) 223.
[33] C. C. Gerry, J. Mimih, Contemp. Phys. 51 (2010) 497.
[34] X. X. Xu, H. C. Yuan, Int. J. Theor. Phys. 53 (2014) 1601.